Lasers in Manufacturing Conference 2023

In-situ laser heat treatment during laser beam welding of dual-phase steels

Martin Dahmen, Rebar Hama-Saleh Abdullah, Dora Maischner, Patrick Meyer*, Alexander Olowinsky

Fraunhofer-Institute for Laser Technology, Steinbachstrasse 15, 52074 Aachen, Germany

Abstract

During laser beam welding of dual-phase steels with tensile strengths above 780 MPa premature weld failure has been detected. Local embrittlement and the formation of micro-cracks are assumed to be possible reasons for the failure. Local in-situ heat treatment has been applied using laser radiation with the aim to soften fused zone and the fusion line area and, simultaneously to rise hardness in the tempering zone. Trials were undertaken to test the feasibility of laser heat treatment at feed rates typical for laser beam welding of thin sheet metal of DP980 in two gauges and from two manufacturing routes. The power density as well as the stand-off were varied to reveal the effects of utilising the weld heat for the heat treatment. The results indicate the possibility to reduce the hardness in fused zone and coarse-grain zone whereas the tempering zone tends to broaden depending on the power applied for laser heat treatment.

Keywords: Laser beam welding; laser heat treatment; heat-affected zone; dual-phase steel softening

1. Introduction

Utilising lightweight construction concepts, ultra-high-strength steels with tensile strengths above 1 GPa are increasingly used in vehicle engineering and other applications. These are also increasingly used as a component of so-called Tailor Welded Blanks (TWB) and Tailor Welded Coils (TWC). One of these advanced high-strength steels are dual phase steels with yield strengths of up to 900 Mpa.

The foundations for the development of these steels were laid in the 1970s. By embedding martensite in a ferritic matrix, high strengths at high elongations at fracture with a high elongation reserve are achieved. For their production, steels with ferritic-pearlitic or ferritic-bainitic microstructure are partially austenitised by heating to the intercritical range followed by quenching to below martensite starting temperature, tempering, and cold rolling. The alloying elements and the control of the temperature and cooling rate

determine or adjust the martensite content and grain size, and thus the mechanical properties (Taşan et al. 2015, Davies 1978). Dual-phase steels are used in strength classes from 400 to 1280 MPa tensile strength. Due to their microstructure, these steels have excellent forming properties. Fracture of the unwelded material occurs after flow of the ferrite phase in conjunction with coagulation of defects between ferrite and martensite (Wei et al. 2015). Fractures in the martensite islands have also been observed (Gould et al. 2006).

Laser-welded joints show a different cracking behaviour resulting from the thermal effect of the joining process. Up to a tensile strength of 600 MPa, dual-phase steels show excellent suitability for fusion welding. With increasing carbon content or increasing strength, different zones appear in the weld area. The weld metal with high hardness is followed in the heat-affected zone by a narrow area with very high hardness at the beginning of the coarse grain zone. This is followed by a drop in hardness below the level of the base metal before the hardness of the base metal is reached after a shallow rise, which can also have a local hardness maximum. Fracture occurs normally in the tempered zone where the strength is reduced (figure 1 a2). Under some circumstances failure originates in the coarse-grained zone (CGZ) near the fusion line. The failure path starts from an embrittled area leading to a micro-crack at the bottom part of the CGZ and deviates into the weaker parts of the weld zone.

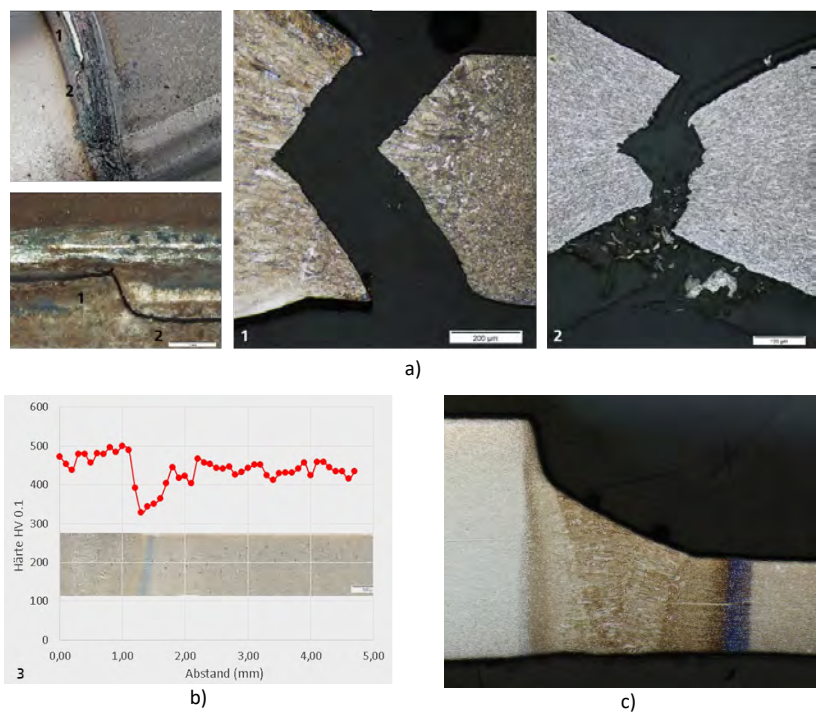

Fig. 1. (a) Fractures in the weld zone of a DP980 in view and micro-section, (a0) view of a top bead with crack and ply change, (a1) fracture in the weld with exit at the fusion line, (a2) ductile fracture in the tempering zone (b) hardening progression in the weld zone, and (c) intact weld in conjunction with an S500 mild steel.

Figure 1 a0 and a1 show typical failure patterns in top view and cross-section, respectively. On way to overcome this type of failure is to restore ductility in the critical zone by subsequent heat treatment utilising the weld heat as the basic heat source. It has to be shown that the properties of the weld can be improved as well as this technique can be facilitated an in-line heat treatment, e.g. in welding tailored strips.

2. State of the art

Short time tempering is a technique applied for economic heat treatment. Undesired effects of conventional tempering as temper embrittlement shall be avoided using short thermal cycles. The technique itself as well as its effects has been applied to a range of materials and is still under investigation. Applying rapid tempering of an AISI 4340 (1.6565) for 1 second compared to 1 hour soaking time varying the Hollomon-Jaffe Parameter (TP) led to an improvement of the impact energy at TP > 9000 while hardness was affected insignificantly (Euser et al. 2020). Laser heat treatment processes have been investigated regarding the local softening of blanks made of martensitic and dual-phase steels in several papers (Keskitalo et al. 2007, Neugebauer et al. 2009, Heyde et al. 2010, Bergweiler 2013). It was shown that local heat treatment by means of laser radiation can significantly improve the formability of ultra-high-strength cold-forming steels with tensile strengths up to more than 1200 MPa. The softening is based either on the tempering of the martensite or the austenitisation with subsequent slow cooling. DP 1180 reacts from a temperature of 450 °C with a decrease in strength. From about 830 °C, a slight recovery occurs (Lapouge et al. 2019). In tests on DP980, a coagulation of the martensite as well as a reduction in grain size and an increase in hardness with increasing processing speed due to increased cooling rates could be observed (Kong et al. 2009). The process improved the formability and avoided drawing cracks (Capello & Previtali 2007). In investigations on inductive tempering of welds in DP800, no influence of inductive heat treatment on the mechanical properties could be found [Bormann 2004]. The reason for this is the annealing temperature of 400 °C, which is too low. Changes in short-time tempering only occur above 500 °C (Baltazar Hernandez 2011, Kamp et al. 2012, Jahn 2011). Investigations into heat treatment with laser radiation on DP800 and DP1200 led to a failure in the tensile test in the weld. The cause is assumed to be the strongly directionally solidified microstructure, caused by a high yield energy during welding.

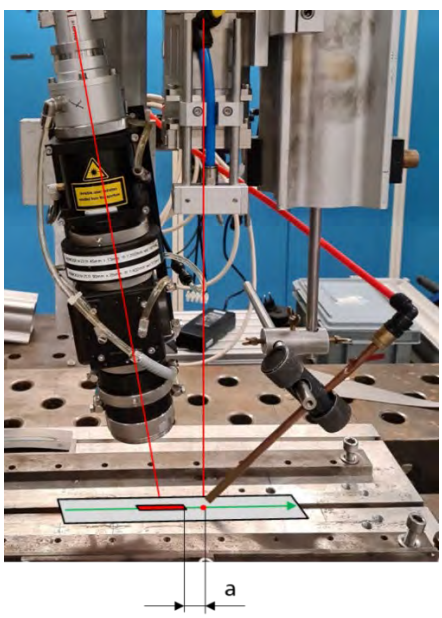

a) Optics set-up with the welding heat (right) and the heat treatment optics (left)

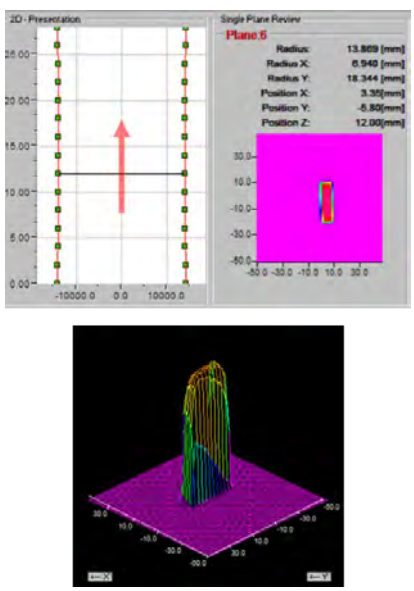

b) Intensity profile of the heat treatment beam

Fig. 2. Experimental set-up and beam parameters of the heat treatment beam.

In investigations of the yield bending properties of welded high-strength low-alloy steels before and after multiple heat treatment, it was shown that laser heat treatment has a positive effect on the forming capacity. In bending tests, smaller radii could be achieved without cracking when bending by 90°.

Non-isothermal annealing at 600 and 700 °C led to a significant reduction of hardness in the weld and to a clear improvement of the forming properties. The forming properties of welded joints are thereby investigated and evaluated by means of tensile tests, bending tests and Nakajima tests (Luo et al. 2019).

3. Experimental

For the trials a combined optics head consisting of a welding optics using standard focusing and a rectangle-shaped beam were used. The welding head was mounted stiffly to the robot hand whereas the position (stand-off a in figure 2a) and the inclination of the heat treatment head could be varied with respect to the former. For the welding task a disk laser beam to a diameter of 506 µm. Its beam was delivered by a fibre of 200 µm in diameter and shaped by a collimator and a focusing lens of 158 mm and 400 mm, respectively. For heat treatment a diode laser has been applied. Beam shaping was realised by two transmissive integrator lenses followed by focusing through standard lenses. A rectangular beam profile of dimensions 37×13 mm^2 was achieved in the focal plane. With the length of the beam in focal plane a retardation of cooling of 0.6 s is obtained. The inclination was set to 20° whereas the stand-off has been varied.

Welding speed was set to 4 m/min, beam power was adjusted to attain a sound full penetration depending on the sheet thickness t, i.e. 1200 W in case of t = 0.9 mm and 2500 W in case of t = 1.5 mm. The power for the heat treatment has been varied from 1200 to 5000 W. The welding beam was positioned orthogonally to the sheet surface. For reasons of accessibility the heat treatment beam was inclined by 20° with respect to the welding beam in trailing or leading arrangement.

Table 1: Characterisation of the materials under investigation. Chemical analysis given in mass-percent.

Material	t/mm	Condition	C	Si	Mn	Cr+Mo	Nb+Ti	V	Al	Cu
DP980-1	0.9	HR uncoated	0.13	0.20	1.90	0.19	0.02	<0.01	0.04	0.01
DP980-2	1.5	CR Zn-coated	0.074	0.24	2.45	0.39	0.04	<0.01	0.16	0.31

For the experiments two different kinds of dual phase steels DP980 (1.0944) were under investigation. DP980-1 is a hot rolled sheet material delivered as uncoated with a thickness of 0.9 mm. DP980-2 has a thickness of 1,5 mm and was delivered zinc-coated. This coating was removed for the trials by pickling in HCl and sandblasting, respectively. Table 1 comprises the chemical composition of the steels under investigation in mass percent measured by optical emission spectroscopy. Both materials have been produced by the thermal route only. In case of DP980-1 the dual-phase structure was verified by a LePera etch. The martensite content varies between 35 and 37 percent by area.

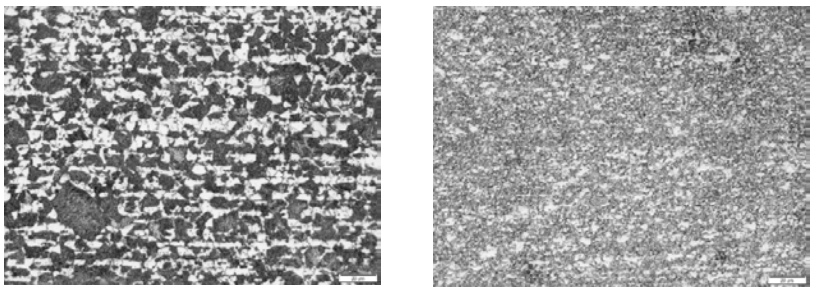

a) DP980-1 b) DP980-2

Fig. 3. Microstructures of the Dual-phase steels under investigation as delivered.

In figure 3 the microstructures of the materials as delivered are depicted. Both materials show a clear ferritic-martensitic microstructure. The mean ferrite grain size of the DP980-1 is 6 µm with a clearly visible separation of different lines with different martensite content. The DP980-2 shows a more finely dispersed mixing of the phases with a mean grain size of 4,5 µm and slightly coarser ferrite grains.

Trials were undertaken with the aim to obtain a constant hardness profile across the weld zone. Minimum condition is to avoid the local hardness increase at the fusion line. In order to get an insight in the behaviour of process and materials the effects of the following parameters were investigated:

- initial temperature (20°C, 800°C, 600°C, 430°C) by varying the stand-off a,
- zinc coating (at DP980-2 only),
- sheet thickness t, and
- trailing/leading position of the heat treatment beam (a = 30 – 70 mm, a = -15 mm).

The starting temperatures have been determined by thermal simulations of the welding as well as the complete process.

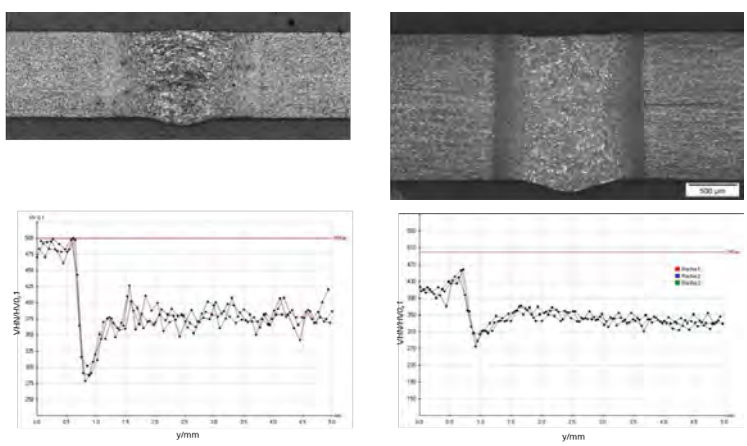

a) DP980-1: b) DP980-2

Fig. 4. Macro-sections and hardness profiles of the seams in as-welded condition. Hardness is measured with a test load of 0,098 N. The red constant line represents the 500 HV0,1 level. Base metal hardness 380 HV0.1 (average).

Evaluation of the welds is carried out by micro-hardness measurements with test loads of 0.981 N and 9.81 N (HV 0.1 and 1) with emphasis on the fused zone, the CGZ near the fusion line, the temper zone, and, if existent, the area of re-hardening at the transition from temper zone to base material. Measurements

with lower test load were used to localise the transition points in the heat affected zones. Measurements with HV1 were made afterwards at these positions. The difference in the indication with both test loads was assessed in preliminary measurements and was found to be 25 to 30 HV at test load 9.81 N (HV1) lower compared to the indication at test load 0.981 (HV0.1). Within the frame of metallographic inspection the root causes for the changes in hardness were investigated on a microstructural level.

In figure 4 the macro-sections of the seams in both steels in as-welded conditions are shown. The DP980-1 shows a small step in the hardness profile in the fused zone and on the fusion line with a slight increase from 485 to 500 HV0.1, respectively. In the temper zone hardness is reduced to 285 HV0.1. There is a pronounced re-hardening zone beside the temper zone with peak values of about 410 HV0.1. The weld in material DP980-2 shows a clear difference in hardness in fused zone and fusion line of 415 and 470 HV0.1, respectively. Hardness of the temper zone is the same as for the DP980-1. Re-hardening is less pronounced and leads to a hardness of about 370 HV0.1.

4. Results and discussion

1.1. 4.1 Material DP 980-1

In figure 5 the resulting hardness profiles after ex-situ and in-situ heat treatment are depicted. The dashed black line corresponds to the state without any treatment. The graph in figure 5a shows that there is no difference at a beam power of 1200 W on the cold specimen. An effect is only visible from 2400 W on where the hardness is reduced to 350 HV1 and to 310 HV1 when power is increased to 3600 W. Utilising the welding heat (figure (figure 5b) a hardness reduction is visible from the lowest power setting at 1200 W on. The effect on hardness reduction appears to be less pronounced. It is assumed that at the stand-off a = 30 mm the material is held at a temperature in the inter-critical range or above. The slight reduction in hardness with increasing beam power can be explained by slower cooling in the thinner sheet metal.

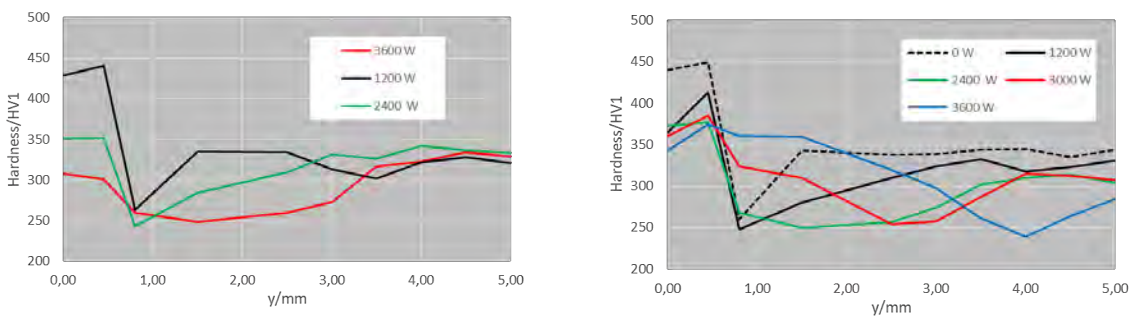

a) Heat treatment ex-situ, specimen temperature 22°C

b) Heat treatment in-situ. Stand-off a = 30 mm

Fig. 5. Graphical comparison of the different heat treatment techniques.

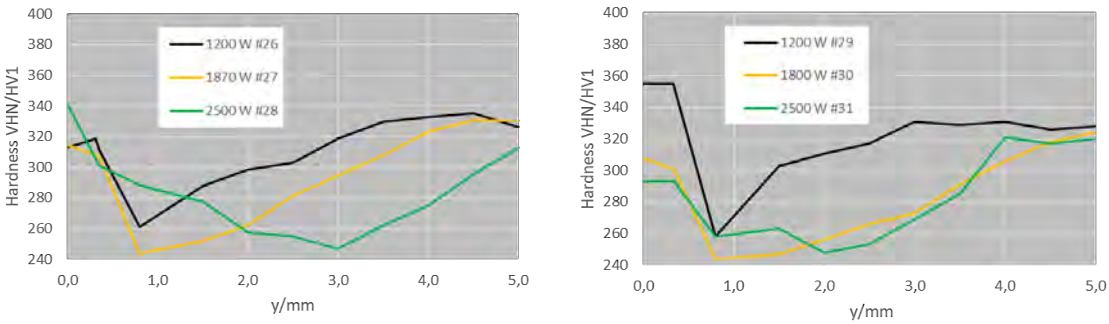

a) Stand-off a = 50 mm. b) Stand-off a = 70 mm

Fig. 6. Effect of the stand-off and the start temperature for heat treatment 600°C (a) and 430°C (b).

Increasing the stand-off leads to a decrease of hardness in fused zone and on the fusion line. At a = 50 mm and an estimated start temperature below A_{c1} the hardness levels amount to 315 to 340 HV1 (figure 6a). A further decrease is obtained at a = 70 mm where the starting temperature corresponds with the bainite nose (figure 6b). The high level for the beam power of 1200 W indicate that the weld temperature was too low at starting of the heat treatment. Increasing the power leads to a decrease of minimum hardness in the temper zone by approximately 20 HV1 which corresponds to the value for the alloy in normalised state. Also, a widening of the temper zone and its slight outward shift can be observed.

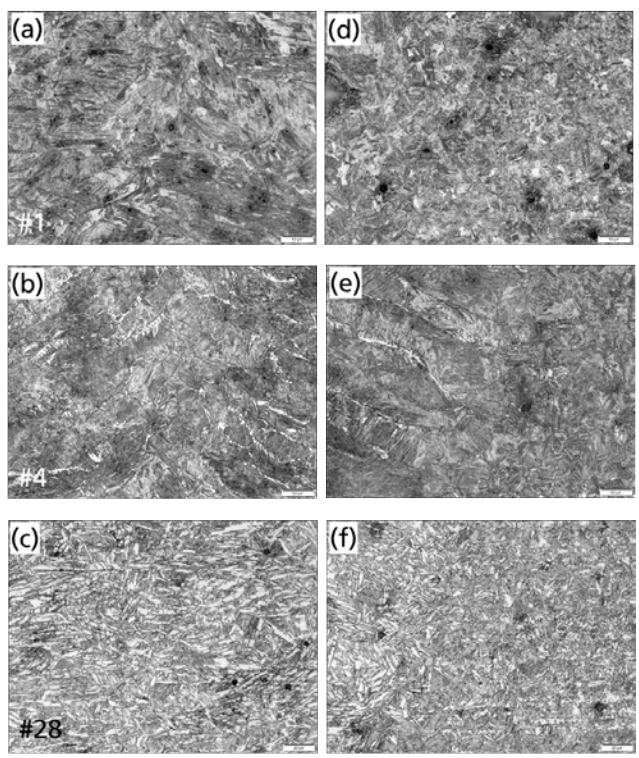

Fig. 7. Micrographs of welds in DP980-1 at the weld centre line (left column) and the coarse-grained zone (right column)- (a) and (d) as-

welded, (b) and (e) stand-off a = 30 mm, beam power 2400 W, (c) and (f) stand-off a = 50 mm, beam power 2500 W.

Micro-sections were taken from the weld centre line and the fusion line to the coarse-grained zone. In Figure 7 the respective microstructures are displayed for varying heat treatment power and different stand-offs. If no treatment is applied the weld centre line has a bainitic-martensitic microstructure where the martensite is distributed in small islands visible from local over-etching (limited black spots or areas) (figure 10 a). A concentration of these martensitic island can be seen at the fusion line (figure 10d) on the solid border. They may act as sources of embrittlement and premature failure on loading. Figures 10 b and e show the structures after in-situ heat treatment with 2500 W at stand-off of 30 mm. In the weld centre it is bainitic but showing some streaks of retained austenite at the grain boundaries. This indicates a maximum temperature of above A_{c3} in conjunction with fast cooling. At the fusion line the martensite islands disappeared, only one micro-void is left. Increasing the stand-off to 50 mm leads to a bainitic-ferritic microstructure throughout the fused zone. Also, the area around the fusion line is well homogenised. Some micro-voids are still visible under the optical microscope.

1.2. 4.2 Material DP 980-2

The material DP980-2 is delivered in 1.5 mm thickness and zinc coated. In a first trial the effect of the coating was tested. For the remaining trials the coating was removed by pickling with hydrochloric acid. A comparison of the hardness profiles shown in figure 8 reveals the effect of the coating. Stand-off was set to 30 mm in this experiment. Black curves show the hardness profile in untreated condition. With the onset of heat treatment hardness levels are comparable in both material states up to 3780 W beam power of the heat treatment laser beam. In the coated sheet any effect is constrained to the fused zone as this has a larger absorptivity compared to the coating. In the temper zone neither hardness value nor its position is affected. In all test runs the coating remained on the surface although after the experiments with high power above 3780 W traces of melting have been observed. If the coating is removed the effect of heat treatment spreads of a wider area (figure 8b). Despite of the reduction of hardness at the fusion line its maximum values remain unchanged. Minimum values in the temper zone are also unchanged but shifted outwards. This leads to the conclusion that processing temperatures at this stand-off reach an inter-critical value at only slightly longer cooling times maintaining the hardness instead of softening the weld zone. Thermal simulation confirmed a starting temperature for heat treatment of 750°C which is at the lower boundary of the inter-critical temperature interval.

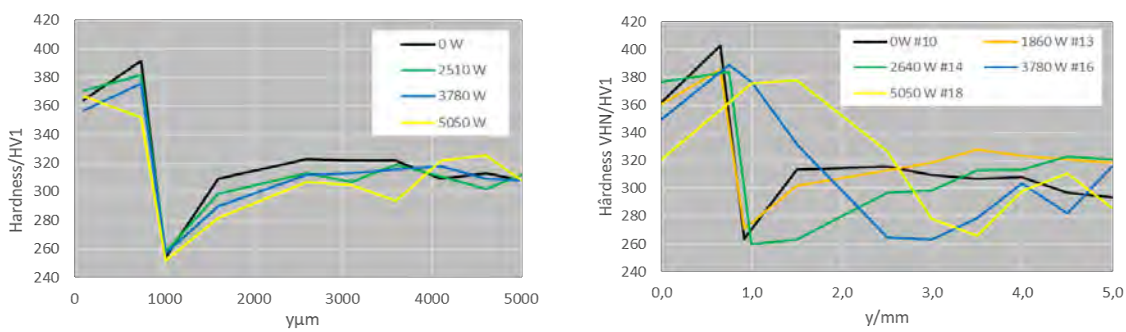

a) Zinc-coated sheet material

b) Uncoated (pickled) material

Fig. 8. Hardness profiles illustrating the effect of the coating on the material DP980-2.

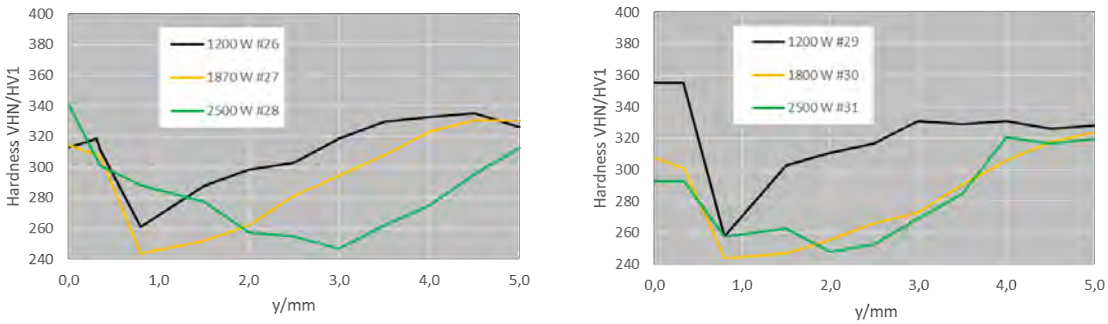

a) Stand-off a = 50 mm b) Stand-off a = 70 mm

Fig. 9. Hardness profiles after heat treatment at longer stand-offs

As the effect is independent of the beam power applied in heat treatment the stand-off between the beam was increased, to 50 mm and to 70 mm, corresponding to a starting temperature of 600°C and 430°C, respectively. Figure 9 displays the hardness profiles at increased stand-off or lower starting temperature. A significant effect can be observed for a = 50 mm. Even at the lowest power of the heat treatment beam hardness in fused zone and at the fusion line is reduced by almost 100 HV1 although a little peak at the fusion line still exists but is negligible. This peak disappears at a beam power of 1870 W. At 2500 W obviously a certain re-hardening of the fused zone takes place. The opposite holds true for a stand-off of a = 70 mm. Here the decrease of hardness at 1200 W is not very pronounced whereas at higher beam power a significant decrease in hardness as well as a widening of the temper zone occur.

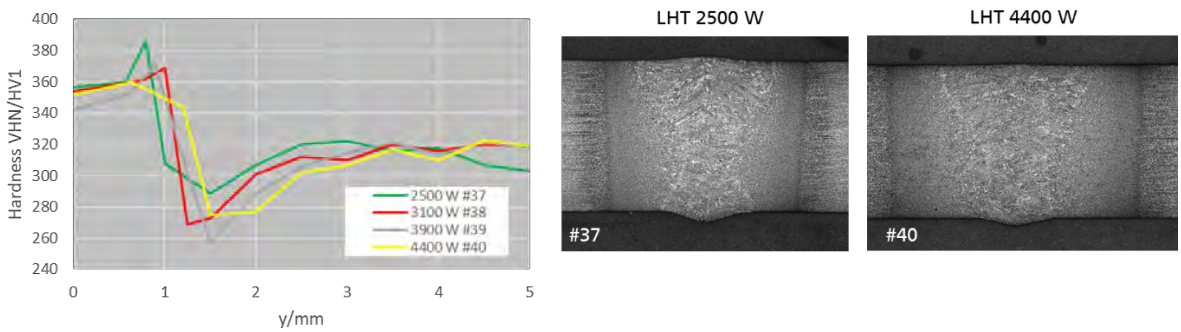

a) Stand-off a = -15 mm b) Macro-sections with 2500 and 4400 W beam power

Fig. 10. Hardness profiles and macro-sections after heat treatment in leading position

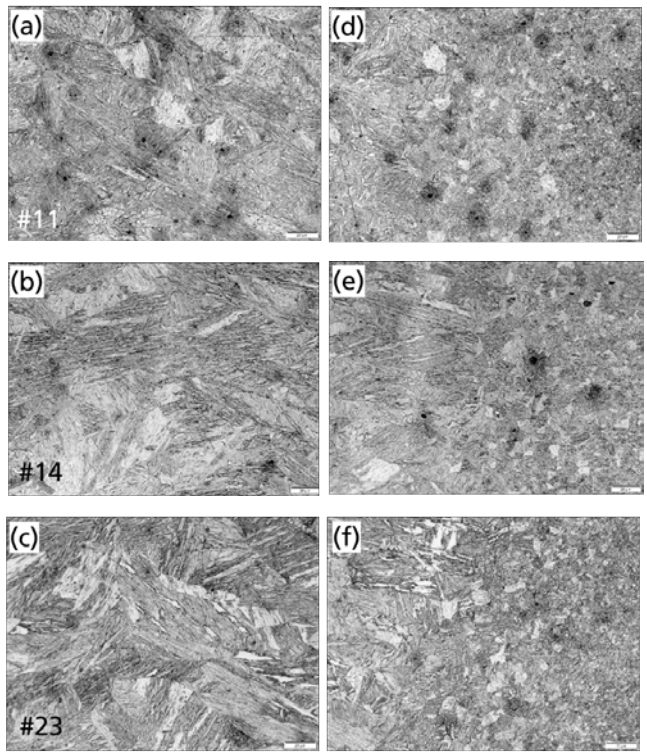

Fig. 11. Micrographs of welds in DP980-2 at the weld centre line (left column) and the coarse-grained zone (right column) - (a) and (d) as-welded, (b) and (e) stand-off a = 30 mm, beam power 2400 W, (c) and (f) stand-off a = 50 mm, beam power 2500 W.

To test the effect of preheating a test on DP 980-2 with a leading heat treatment beam was conducted. The results are shown in figure 10. It is obvious that a significant change in the peak hardness occurs only at quite high beam power of 4400 W. Also, a wider seam can be observed as a consequence of the leading heat input. The macro-sections in figure 10b show the increase of seam width and heat-affected zone and correspond well with the hardness profile in figure 10a. For this experiment the coating has been removed by sandblasting. Hence, an increased absorptivity should be expected (Hipp et al. 2019, Bergstrom et al. 2007). Even under an assumed higher absorptivity the leading position was proven to be less effective under the conditions given.

The fused zone in as-welded condition displays a bainitic microstructure as shown in figure 11a. Tiny over-etched dots indicate some martensite at the column boundaries. These are also found in the coarse-grained zone but, in contrast to material DP980-1, not lined up at the fusion line (figure 11d). Austenite has not been found in any of the welds. At the stand-off of 30 mm no change in microstructure, neither in the fused zone nor at the fusion line, can be stated (figure 11 b and e). Heat treatment seems to be ineffective under this condition. Increasing the stand-off leads to a certain coarsening of the bainitic structure in the fused zone. In both areas not any martensite islands are visible (figure 11 c and f). No retained austenite has been observed.

5. Conclusions

Experiments on in-situ laser heat treatment during laser beam welding were reported. Under the parameters of the heat treatment beam given a stand-off of 30 mm (trailing) and -15 mm (leading) there are no effects of the treatment visible. The temperature reaches the inter-critical region above A_{c1}, partially even A_{c3} leading to a general hardening in the fuses zone and the CGZ but increasing the temper zone. A significant decrease in hardness as well as a reproducible process were determined at a stand-off of 50 mm in the case of DP980-1 and 70 mm in the case of DP980-2. The effective beam power for heat treatment amount to 1200 – 1500 W and 1800 – 2500 W, respectively.

Table 2: Overview over hardness and microstructure of DP980-1 after heat treatment at 2500 W. Microstructure is denoted as B – bainite, F – Ferrite, M – martensite, and RA – retained austenite.

Start temperature/°C		20	800	600	430
Stand-off a/mm		-	30	50	70
HVN/HV1	Fused zone	350	350	340	280
	Fusion line	350	375	300	280
	Temper zone	245	270	240	250
Microstructure		B + M	B + RA	B	B + F

Tables 2 and 3 show a comparison of the effects of heat treatment for both materials. It seems that DP980-1 works a bit harder and has a less uniform microstructure in the fused zone compared to DP980. The reason for this is assumed to be the more inhomogeneous distribution of the martensite in the base material of the former material.

Table 3: Overview over hardness and microstructure of DP 980-2 after heat treatment at 2500 W. Microstructure is denoted as B – bainite, F – Ferrite, M – martensite, and RA – retained austenite.

Start temperature/°C		20	800	600	430
Stand-off a/mm		-	30	50	70
HVN/HV1	Fused zone	380	380	350	330
	Fusion line	380	390	355	320
	Temper zone	260	260	275	275
Microstructure		B + M	B + M	B	B

A Zn coating limits the effects of heat treatment but offers the opportunity to restrict the effects onto the interesting areas, i.e. the fused zone and the fusion line. To increase the efficiency of the process a narrower and longer heat treatment beam can be applied. Especially when at industrially applied welding speeds of approximately 9 m/min and elongation is required in order to ensure the heat treatment of the full weld to the most vulnerable points at the root.

Further investigation of the mechanical properties and the forming behaviour will follow to verify the benefits of in-situ heat treatment. Also, the development of tools for a full laser-integrated solution is an ongoing matter of research and testing.

Utilising welding heat in conjunction with an increase absorptivity of the heat of welding makes this technique feasible to overcome local embrittlement. Applications are seen in the production of straight square butt welds, as in tailored strip manufacturing, an in certain limits in two-dimensional welding of

tailored blanks with curved welds. The results established at dual phase steels give rise for application on other martensite phase steels.

References

Baltazar-Hernandez, VH, Nayak, SS, Zhou, Y (2011): Tempering of martensite in dual-phase steels and its effects on softening behavior, *Metallurgical and Materials Transactions* A 42, 3115–3129

Bergweiler, G (2013): *Lokale Wärmebehandlung mit Laserstrahlung zur Verbesserung der Umform- und Funktionseigenschaften von hochfesten Stählen*, Dissertation RWTH Aachen

Bergström, D, Powell, J, Kaplan, A (2007): The absorptance of Nd:YLF and Nd:YAG laser light at room temperature. *Applied Surface Science*, 253, 5017-5028

Euser, VK, Clarke, AJ, Speer, JG (2020): Rapid tempering: Opportunities and challenges. *Journal of Materials Engineering and Performance* 29(7), 4155-4161, doi: 10.1007/S11665-020-04946-z

Borman, A (2004): *Serielle, induktive Wärmebehandlung laserstrahlgeschweißter Feinbleche*, PhD thesis, Hannover

Bräutigam-Matus, K, Altamirano, G, Salinas, A, Flores, A, Goodwin, F (2018): Experimental determination of continuous cooling transformation (CCT) diagrams for dual-phase steels from the intercritical temperature range. *Metals* 8, 674 (2018), doi:10.3390/met8090674

Capello, E, Previtali, B (2007): Enhancing dual phase steel formability by diode laser heat treatment, *ICALEO, Laser Materials Processing Conference Vol. 26* , 251-260

Davies, RG, (1978): Influence of martensite composition and content on the properties of dual phase steels, *Metallurgical Transactions* 9A, 671-679

Gould, J.E., Khurana, E.P., Li, T. (2006): Predictions of icrostructures when welding automotive advanced high-strength steels, *Welding Journal Research Supplement*, Issue 5, 111–116

Heyde, M., Roll, K., Kawalla, R., Bergweiler, G., Kaiser, J. (2010): Local heat treatment of ultra-high-strength steels - an opportunity to extend the range of car body components, *IDDRG International Conference*J

Hipp, D, Mahrle, A, Beyer, E (2019): Beyond Fresnel: absorption of fibre laser radiation on rough stainless steel surfaces. J*ournal of Physics D: Applied Physics* 52, 355302

Jahn, A (2011): *Umformbarkeit laserinduktionsgeschweißter Strukturen aus höherfesten Stahlfeinblechen*, Dissertation, Dresden

Kamp, A, Celotto, S, Hanlon, DN (2012): Effects of tempering on the mechanical properties of high strength dual-phase steels, *Materials Science and Engineering* A 538, S. 35-41

Keskitalo, M, Mäntyjärvi, K, Mäkikangas, J, Karjalainen, JA, Leiviskä, A, Heikkala, J (2007): Local laser heat treatments of ultra-high strength steel, Proceedings 11th NOLAMP, *Nordic Conference in Laser Processing of Materials*, 11, Lappeenranta, FI, 20-22 August, 536-546

Kong, F, Santhanakrishnan, S, Lin, D, Kovacevic, R (2009): Modeling of temperature field and grain growth of a dual phase steel DP980 in direct diode laser heat treatment. *Journal of Materials Processing Technology* 209, 5996-6003

Lapouge, P, Dirrenberger, J, Coste, F, Schneider, M (2019): Laser heat treatment of martensitic steel and dual-phase steel with high martensite content. *Materials Science and Engineering* A 752, 128-135, doi: 10.1016/j.msea.2019.03.016

Luo, C, Cao, Y, Zhao, L, Shan, J (2019): Laser heat treatment of low-alloy ultrahigh-strength steel laser-welded joints, *Welding Journal Research Supplement*, Issue 8, 227s-240s, doi: 10.29391/2019.98.020

Neugebauer, R, Scheffler, S., Poprawe, R, Weisheit, A (2009): Local laser heat treatment of ultra high strength steels to improve formability, *Production Engineering* 3, 347-351

Speich, GR, Leslie, WC (1972): Tempering of steel. *Metallurgical Transactions* 3, 1043-1053

Taşan, C, Diehl, M, Yan, D, Bechtold, M, Roters, F, Schemmann, L, Zheng, C, Peranio, N, Ponge, D, Koyama, M, Tsuzaki, K, Raabe, D (2015): An overview of dual-phase steels, *Annual Review of Materials Research* 45, 391–431

Wei, C, Zhang, J, Yang, S, Tao, W, Wu, F, Xia, W (2015): Experiment-based regional characterization of HAZ mechanical properties for laser welding, *International Journal of Advanced Manufacturing Technology* 78, 1629–1640